Journal of Solid State Chemistry 181 (2008) 3086–3094

Contents lists available at ScienceDirect

Journal of Solid State Chemistry

journal homepage: www.elsevier.com/locate/jssc

# Optimum conditions for intercalation of lacunary tungstophosphate(V) anions into layered Ni(II)–Zn(II) hydroxyacetate

M. Angeles Ballesteros [a], M. Angeles Ulibarri [a], Vicente Rives [b], Cristobalina Barriga [a,*]

[a] Departamento de Química Inorgánica e Ingeniería Química, Universidad de Córdoba, Campus Universitario Rabanales, Edificio Marie Curie 1ª Planta, 14071 Córdoba, Spain
[b] GIR-QUESCAT, Departamento de Química Inorgánica, Universidad de Salamanca, Salamanca, Spain

ARTICLE INFO

*Article history:*
Received 1 April 2008
Received in revised form
16 July 2008
Accepted 20 July 2008
Available online 9 August 2008

*Keywords:*
Layered materials
Hydroxyacetate
Intercalation
Tungstophosphate(V)

ABSTRACT

Acetate containing nickel–zinc hydroxysalts (LHS-Ni–Zn) have been synthesized by coprecipitation and hydrothermal treatment. The acetate anions were exchanged with $PW_{12}O_{40}^{3-}$ anions, and optimum conditions to attain the maximum level of W in the compound have been identified. The W intercalated compound was characterized by powder X-ray diffraction, FT-IR spectroscopy, thermogravimetric and differential thermal analyses, scanning electron microscopy and transmission electron microscopy.

The exchange of LHS-Ni–Zn with $PW_{12}O_{40}^{3-}$ at pH = 3 for 72 h leads to a solid with a basal spacing of 9.62 Å and a W content (weight) of 37%. The hydrothermal treatment at 90 °C for 24 h increases this value to 48% with a W/Zn molar ratio of 1.38, which corresponds to a layered compound with lacunary tungstophosphate anions in the interlayer space. The intercalated solid is stable up to 250 °C, the layer structure collapses on dehydroxylation and amorphous compounds were identified at 500 °C. Two crystalline phases, NiO (rock salt) and a solid solution $(Zn_{1-x}Ni_x)WO_4$, were identified by powder X-ray diffraction at high temperature (ca. 1000 °C).



## 1. Introduction

Among the compounds with the layered double hydroxides structure (LDH), the so-called hydrotalcite-like compounds have been widely studied [1–3], while the layered hydroxide (or basic) salts (LHS) with a similar structure have not been studied in such details [4,5]. Layered hydroxide salts exhibit exchange properties [6–8] and the intercalation of different anions into these compounds can be an alternative way to obtain oxides and mixed oxides with specific composition and properties.

The (Ni, Zn)-hydroxyacetate with the general formula $Ni_{1-x}Zn_{2x}(OH)_2(CH_3COO)_{2x}\cdot nH_2O$ is built in layers of $Ni(OH)_2$ with the brucite structure; when $x Ni^{2+}$ cations are removed from the layers, the resulting negative charge is extrabalanced by $2x$ $Zn^{2+}$ cations located at tetrahedral sites on both sides of the empty octahedral hole. The resulting excess of positive charge is definitively balanced by acetate anions located in the interlayer space, where water molecules also exist. At first sight, the differences between hydroxyacetates and hydrotalcite are the absence of trivalent metal cations in the layers and the presence of divalent metal cations in tetrahedral sites on both sides of the layers in the former compounds. These structural features provide a different environment of the interlayer species, specially because $Zn^{2+}$ cations are more exposed to external reagents and their tetrahedral coordination (with three hydroxyl groups of the layers) is completed with the interlayer anion and/or interlayer water molecules. A schematic representation is included in Fig. 1. Because of these special characteristics, a new kind of reactivity in LHS may be expected.

On the other hand, polyoxytungstate anions are very interesting for their photocatalytic applications [9–11]; one of the most important applications developed in the last few years is their use as catalysts in the degradation of dyes and organic pesticides in aqueous systems [12,13]. The equilibrium adsorption on different supports ($TiO_2$, $SiO_2$ and $Al_2O_3$) of the $[PW_{11}O_{39}]^{7-}$ anion from aqueous solutions has been studied [14], concluding that the characteristics of the solute–support interaction are greatly influenced by the nature of the support. In addition, the authors report that during the impregnation of $[PW_{12}O_{40}]^{3-}$ anions, partial hydrolysis can lead to lacunary $[PW_{11}O_{39}]^{7-}$ species, due to the narrow pH range in which the 12-tungstophosphate anion is stable.

Previous papers have reported the high photocatalytic activity of polyoxometalate-containing hydrotalcite and of their thermal decomposition products, to degrade aqueous organochlorine pesticides [13–21]. By analogy to LDH compounds [3] and due to the basic properties of the precursor here used (LHS), as well as the dependence of the polyoxotungstate equilibrium on the pH, synthesis conditions will be very important to attain a final high exchange level in the incorporation of polyoxometalates into

* Corresponding author. Fax: +34 957 218 621.
*E-mail address:* cbarriga@uco.es (C. Barriga).

0022-4596/$ - see front matter © 2008 Elsevier Inc. All rights reserved.
doi:10.1016/j.jssc.2008.07.037

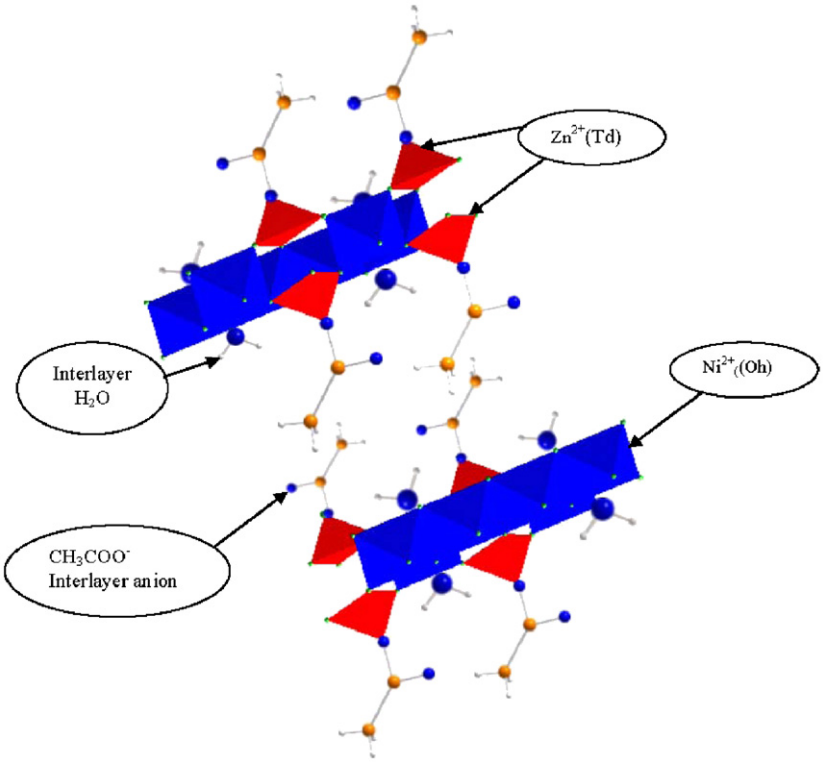


**Fig. 1.** Schematic representation of a (Ni, Zn)-hydroxyacetate structure.

layered hydroxyacetate. One of the many advantages of using these materials is that the cations are homogeneously dispersed in the layers. Consequently, when they are calcined, the mixed oxides formed are well dispersed and, in some cases, formation of solid solutions is rather easy. In addition, the incorporation of polyoxometalates in the interlayer space of hydroxyacetates or hydrotalcite compounds would lead to immobilization of the catalyst, avoiding solubilization (leaching) problems of the catalyst.

The aim of this work is to obtain the optimum conditions for intercalation of polyoxotungstate into a Ni, Zn hydroxyacetate, as well as the study of their thermal stability in order to know the nature of the calcined products at different temperatures.

## 2. Experimental

### 2.1. Ni(II)–Zn(II) hydroxyacetate

The method used to prepare the starting hydroxyacetate sample has been described elsewhere [7]. Aqueous solutions of Ni(II) and Zn(II) acetates (1 M) were mixed in amounts corresponding to a Zn/Ni molar ratio of 0.5. Water used to prepare the solutions was first boiled to remove dissolved $CO_2$. The solution was submitted to hydrothermal treatment at 150 °C for 24 h. The pale green solid was separated by centrifugation. The solid was washed several times with distilled water and dried at room temperature in a vacuum desicator over $P_2O_5$.

All chemicals were from Fluka (Switzerland) and Panreac (Spain) and were used without further purification.

### 2.2. Exchanged sample

A portion (0.5 g) of Ni(II)–Zn(II) hydroxyacetate was dispersed in water (ca. 50 mL) at room temperature for 24 h. An aqueous solution containing $Na_3PW_{12}O_{40}$ (4.5 g) in 50 mL was added with vigorous stirring to the slurry of hydroxyacetate; the pH was pre-adjusted with 0.05 M NaOH and kept constant at 3, 6.5 or 9.5. The resulting greenish yellow suspension was stirred for 24, 48, 72 or 96 h. The product was centrifuged, washed with decarbonated water and dried in air at room temperature or 75 °C. Here these samples are named as NiZnW*X*-*t*, where *X* stands for pH (3, 6.5 or 9.5) and *t* for contact time of polyoxometalate aqueous solution with the parent material (24, 48, 72 or 96 h). In some experiments, the suspension was submitted to hydrothermal treatment at 90 or 120 °C and these samples are referred to as NiZnW*X*-*t*-HT, where HT stands for hydrothermal treatment at a given temperature (90 or 120 °C).

### 2.3. Samples characterization

Chemical analyses for Ni, Zn and W were carried out by atomic absorption spectrometry in an AAS-3100 instrument from Perkin-Elmer and the amount of C was determined on a Euro Elemental Analyze Eurovector instrument. Powder X-ray diffraction (PXRD) patterns were recorded in a Siemens D-5000 instrument, using nickel filtered Cu*K*α radiation ($\lambda = 1.54050$ Å).

The FT-IR spectra were recorded by the KBr pellet technique (1% weight sample: KBr) in a Perkin-Elmer Spectrum One Fourier Transform instrument.

Differential thermal analyses (DTA) and thermogravimetric analyses (TG) were carried out in a Setaram Setsys Evolution 16/18 instrument, in an argon atmosphere at a heating rate of 5 °C/min. Simultaneous analysis of the evolved gases was performed by mass spectrometry using a Pfeiffer Vacuum OmniStar.

Scanning electron microscopy (SEM) micrographs were obtained using a JEOL 6300 instrument; the samples were prepared by deposition of a drop of sample suspension on a Cu sample holder and covered with an Au layer by sputtering in a Baltec SCD005 apparatus.

Transmission electron microscopy (TEM) images were obtained using a JEOL 200CX apparatus. The samples were dispersed in acetone by ultrasound and settled on copper grids covered with a carbon film for examination.

## 3. Results and discussion

### 3.1. Layered Ni–Zn hydroxyacetate

A hydroxysalt with Ni/Zn = 2, corresponding to a value of $x = 0.2$ in the general formula $Ni_{(1-x)}Zn_{2x}(OH)_2(CH_3COO)_{2x} \cdot nH_2O$, was prepared. Chemical analysis data are summarized in Table 1. The Ni/Zn molar ratio in the solid is the same as in the starting solution.

The PXRD pattern included in Fig. 2 is characteristic of a layered compound similar to a Zn basic salt, $[Zn_5(OH)_8(NO_3)_2 \cdot 2H_2O]$, a very strong diffraction line at 6.85° (2$\theta$) is observed, corresponding to diffraction by (001) planes with $d = 12.9$ Å, together with weak peaks at 13.7, 20.6, 33.7, 49.1 and 59.97° (2$\theta$), which can be assigned to reflexions by planes (002), (003), (020), (220) and (040), respectively. These results are consistent with a hexagonal cell with lattice parameters $a = 6.16$ Å and $c = 12.9$ Å. The precise position of the peak, due to diffraction by the basal spacing, changes with the composition of the sample

**Table 1**
Elemental chemical analysis data and metals molar ratios for intercalated samples under different experimental conditions

| Sample | Ni[a] | Zn[a] | W[a] | C[a] | Ni/Zn[b] | W/Zn[b] |
|---|---|---|---|---|---|---|
| NiZn LHS | 32.34 | 18.04 | – | 6.53 | 1.98 | – |
| NiZnW3-24 | 29.39 | 14.9 | 23.26 | 2.84 | 2.19 | 0.55 |
| NiZnW3-48 | 28.93 | 14.33 | 24.42 | 2.27 | 2.00 | 0.65 |
| NiZnW3-72 | 26.18 | 14.25 | 37.14 | 2.08 | 1.97 | 0.93 |
| NiZnW3-96 | 21.00 | 14.08 | 36.87 | 2.12 | 1.78 | 0.91 |
| NiZnW3-72HT90 | 24.75 | 12.28 | 48.11 | 0.60 | 2.25 | 1.38 |
| NiZnW6.5-72 | 27.38 | 16.24 | 28.38 | 2.24 | 1.85 | 0.62 |
| NiZnW9.5-72 | 27.87 | 18.01 | 14.95 | 2.62 | 1.68 | 0.30 |

[a] Weight percentage.
[b] Molar ratio.

[7,21]. The content of interlayer water in the hydroxysalt depends on the hydration conditions, and the basal space can be reduced by 3 Å upon dehydration by heating the sample at 110 °C. This process is reversible, and when the sample remains at room temperature the humidity of the atmosphere is enough to recover the initial value, $d_{001} = 12.9$ Å [22].

The FT-IR spectrum (Fig. 2 inset) shows a broad absorption band centred at 3427 $cm^{-1}$ [$\nu$(OH)], together with absorptions at 1578 and 1406 $cm^{-1}$ corresponding to $\nu_{as}(COO^-)$ and $\nu_s(COO^-)$, respectively, 1343 $cm^{-1}$ [deformation of the methyl group $\delta(CH_3)$], 1019 and 1050 $cm^{-1}$ [rocking of the methyl group $\rho_r(CH_3)$], although this last band can be attributed also to OH-bending modes [23]. The bands observed below 1000 $cm^{-1}$ may be assigned to lattice stretching vibrations. The difference (172 $cm^{-1}$) between the positions of the bands due to modes $\nu_{as}(COO^-)$ and $\nu_s(COO^-)$ confirms the coordination of the acetate species to the metal cation in a monodentate form [24].

The sample is formed by homogeneous platelet-shaped particles with an average size of 2 μm, as shown in Fig. 3a; curling of the particle borders as observed by TEM (Fig. 3b) is indicative of their extreme thinness.

### 3.2. Intercalation of tungstophosphate anion

The structure of anion $PW_{12}O_{40}^{3-}$ is shown in Fig. 4. It consists of an assemblage of $[WO_6]$ octahedra and a central $[PO_4]$ tetrahedron. The $[WO_6]$ units are edge-shared into four $[W_3O_{13}]$ groups to give the $W_{12}O_{36}$ species that constitutes the cage framework and contains the $PO_4$ tetrahedron. The oxygen atoms in the Keggin-structure anions are classified into four groups; in each trimetallic group the $\mu_2$-oxo bridges are usually named $O_c$, while the $\mu_2$-oxo bridges linking the two adjacent trimetallic groups are named as $O_b$. The $\mu_4$-oxo bridges between the central tetrahedron and the trimetallic groups are named $O_a$. The fourth type of oxygen atoms, the terminal one, is bonded only to one metallic atom and is named $O_d$. In aqueous solution, $PW_{12}O_{40}^{3-}$ has a limited stability range, and at pH 1.5–2 it is rapidly (and reversibly) converted to the lacunary $PW_{11}O_{39}^{7-}$ anion, which undergoes degradation to $PW_9O_{34}^{9-}$ at basic pH, as represented in Fig. 4 [23]. For simplicity, $PW_{12}O_{40}^{3-}$, $PW_{11}O_{39}^{7-}$ and $PW_9O_{34}^{9-}$ anions will be here named as PW12, PW11 and PW9, respectively.

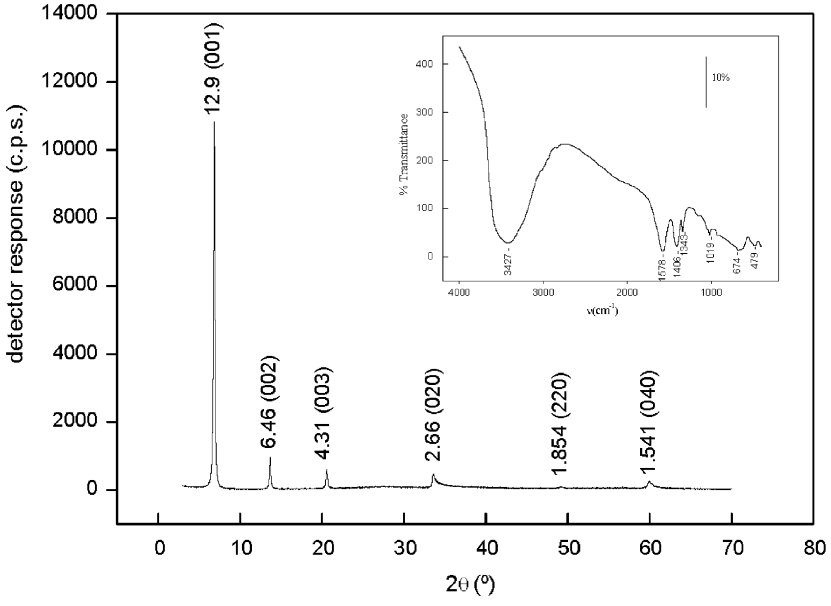


**Fig. 2.** PXRD pattern and FT-IR spectrum (inset) of sample (Ni,Zn)-hydroxyacetate.

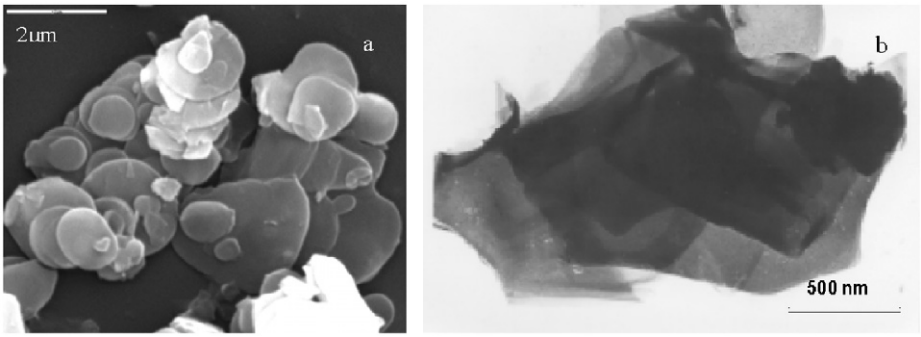


**Fig. 3.** SEM (a) and TEM (b) micrographs of sample (Ni, Zn)-hydroxyacetate.

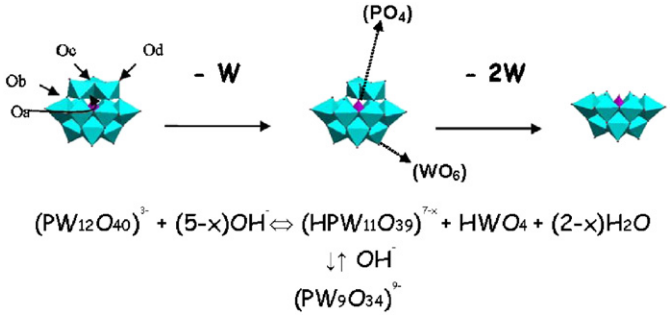


**Fig. 4.** Schematic representation of the $PW_{12}O_{40}^{3-}$ Keggin anion structure and its aqueous equilibrium reactions. $O_a$: $\mu_4$-oxo bridges between the central tetrahedron and the trimetallic groups; $O_b$: $\mu_2$-oxo bridges linking the two adjacent trimetallic groups; $O_c$: $\mu_2$-oxo bridges in each trimetallic group and $O_d$: terminal oxygen atoms bonded only to one metallic atom.

The exchange capacity of layered hydroxysalts with different anions (mono and polyatomic anions with different charges) has been reported in previous papers [7,21]; a kinetic study of the exchange of two organic anions in LHSs has shown a variety of kinetic behaviours, which mostly depend on the relative size of the anions [8].

Here we report the exchange of acetate anions by Keggin anions. The partial hydrolysis of PW12 might take place during the exchange process, leading to the lacunary anions due to the narrow pH range in which PW12 is stable. The effects of different variables such as pH, exchange time, hydrothermal treatment and concentration of the starting $Na_3PW_{12}O_{40}$ salt solution have been studied.

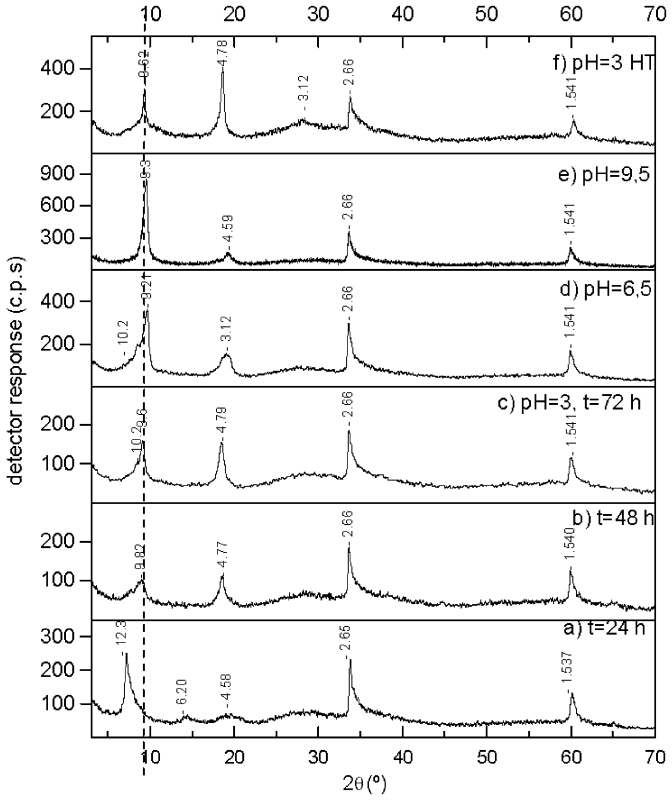


**Fig. 5.** PXRD patterns of samples intercalated with $PW_{12}O_{40}^{3-}$ at different contact times and pH: (a) NiZnPW3-24, (b) NiZnPW3-48, (c) NiZnPW3-72, (d) NiZnPW6.5-72, (e) NiZnPW9.5-72) and (f) NiZnPW3-72HT90. Dashed lines indicate LHS $d_{001}$ spacing.

### 3.3. Effect of exchange time

Several experiments were carried out where the PW12 solution was contacted with the starting LHS for different times at a constant pH of 3. The PXRD patterns of the solids isolated after different contact times are shown in Fig. 5a–c). After 24 h of exchange, the PXRD pattern is similar to the pattern of the precursor sample, with an intense diffraction line at 7.18° ($2\theta$) ($d = 12.3$ Å), but when the time increases to 48 h the PXRD shows two peaks at 12.02 and 9.82 Å in this range. The intensity of the first peak decreases as the contact time increases, and after 72 h the main phase corresponds to a layered compound with $d_{001} = 9.65$ Å, and the peak at lower diffraction angle is recorded simply as a shoulder. Element analysis for these samples shows a progressive increase in the tungsten content from 24 to 72 h, which remains constant after 96 h. On the other hand, an important decrease in the intensities of characteristic bands of acetate anions is observed in the FT-IR spectra (Fig. 6) when the exchange time increases. The bands almost completely disappear after 72 h, which agrees with the largest tungsten content (see Table 1). It has been previously reported [26] that several days at room temperature are needed to reach the equilibrium during exchange reactions on powder Ni–Zn hydroxyacetate samples.

As mentioned above for the hydroxyacetate samples, these types of compounds show basal spacings that critically depend on drying conditions; therefore, all samples were dried at the same temperature (75 °C) to compare the value of $d_{(001)}$. It should be noticed that the FT-IR spectra and the results of chemical analysis for metals do not change after drying the samples at 75 °C. These polyoxometalate-intercalated samples maintained at room temperature in air do not recover the original interlayer spacing as hydroxyacetate salts do, suggesting some sort of anchoring (grafting) of the anion to the layers.

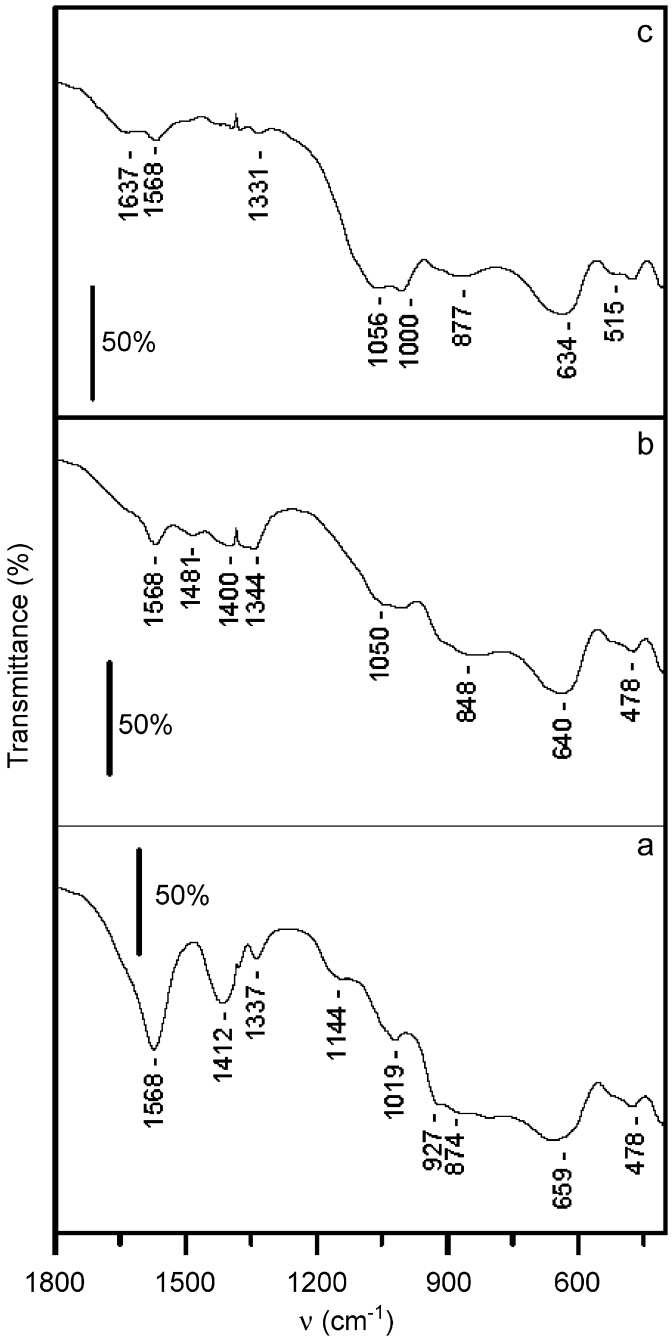


**Fig. 6.** FT-IR spectra (KBr disks) of intercalated (Ni, Zn)-hydroxysalts at different contact times: (a) NiZnPW3-24, (b) NiZnPW3-48 and (c) NiZnPW3-72.

### 3.4. Effect of pH

One of the most important parameters governing the exchange process of anions in LHSs is pH, due to the basic character of the precursor salt and, particularly in the present case, the relative stability of PW12 and its derived lacunary species; actually, the precise nature of PW12 and its derived lacunary species is also pH dependent [9]. The exchange was carried out at different pHs, 3, 6.5 and 9.5, during 72 h. From element chemical analysis data in Table 1, we can conclude that the Ni/Zn molar ratio undergoes a slight decrease after exchange, but the composition of the layer is maintained within the limits of composition of these types of compounds. The tungsten content in the samples decreases as pH increases, indicating a lower content of anions and/or lower nuclearity of the species formed upon partial depolymerization of the anions to give lacunary species, and thus anions such as PW11 or PW9 can be formed [25].

The PXRD patterns of the samples prepared at the tested pH values are shown in Fig. 5c–e. The pattern recorded for the solid prepared at pH 3 corresponds to a layered compound with $d_{001} = 9.65$ Å; this diffraction peak shows a shoulder at 8.48° $2\theta$ ($d = 10.2$ Å). The relative intensity of the peak recorded below 9° ($2\theta$) increases as pH is increased, and it simultaneously shifts to a slightly higher angle; as a result, a rather symmetric peak is recorded at 9.5° ($d = 9.3$ Å) for the sample prepared at pH 9.5.

The FT-IR spectra (not included) show in all cases characteristic bands of acetate anions at 1578 and 1406 $cm^{-1}$ [$\nu_{as}(COO^-)$ and $\nu_s(COO^-)$, respectively], and 1343 $cm^{-1}$ [$\delta(CH_3)$], together with bands between 1100 and 700 $cm^{-1}$ due to tungstophosphate anions. The intensities of these bands depend on the pH value during synthesis; thus, the relative intensities of the acetate bands with respect to the bands due to tungstophosphate increases at high pH, according to the lower W content. This indicates that the exchange reaction is not favoured at basic pHs. These results are confirmed by element analysis data for C included in Table 1.

### 3.5. Effect of hydrothermal treatment

The best conditions to achieve a high level of anion exchange are pH = 3 and contact time 72 h. However, under these conditions the presence of some acetate anions is still concluded from the FT-IR spectra (Fig. 6). To increase the tungsten content, a sample contacted for 72 h with the PW12 solution was submitted to hydrothermal treatment for 24 h at 90 or 120 °C at autogenous pressure in a Teflon-lined stainless steel bomb.

The PXRD diagram of the sample treated at 90 °C (NiZnW3-72HT90), Fig. 5f, shows the first basal diffraction line at 9.3° ($2\theta$) ($d_{001} = 9.62$ Å). Chemical analysis provided a value of 2.28 for the Ni/Zn molar ratio and 1.38 for W/Zn (Table 1). The increase in the Ni/Zn molar ratio suggests a partial dissolution of $Zn^{2+}$, probably due to the extreme synthesis conditions (low pH and high temperature), but the structure still corresponds to a layered compound, similar to the parent hydroxyacetate material, whose PXRD diagram is included in Fig. 2. Additionally, an increase in the W content is observed (Table 1), suggesting that intercalation of the tungstophosphate anions in the interlayer space is easier than without hydrothermal treatment. The FT-IR spectrum of the sample hydrothermally treated at 90 °C shows strong bands between 1100 and 700 $cm^{-1}$ corresponding to Keggin anions, while the intensities of characteristic bands due to acetate anions decrease (Fig. 7), in accordance with the lower C content measured by chemical analysis for this sample, Table 1.

The PXRD pattern (not shown) of the sample hydrothermally treated at 120 °C shows additional diffraction lines to those corresponding to a layered structure, which can be due to a decomposition product of the pursued compound. Consequently, a layered compound with a maximum W content was obtained at 72 h of contact time, pH = 3 and hydrothermally treated at 90 °C.

### 3.6. Effect of concentration of the solution of Keggin species

Although an increase in the concentration of the $Na_3PW_{12}O_{40}$ solution would facilitate the diffusion of tungstophosphate anions into the interlayer space, it has been found that the use of highly concentrated $Na_3PW_{12}O_{40}$ solutions causes dissolution of the hydroxyacetate due to the stronger acidity of the solution.

To avoid this problem and aiming to increase the exchange percentage, the method of successive additions of $Na_3PW_{12}O_{40}$ solution after selected time intervals was tried. The experimental

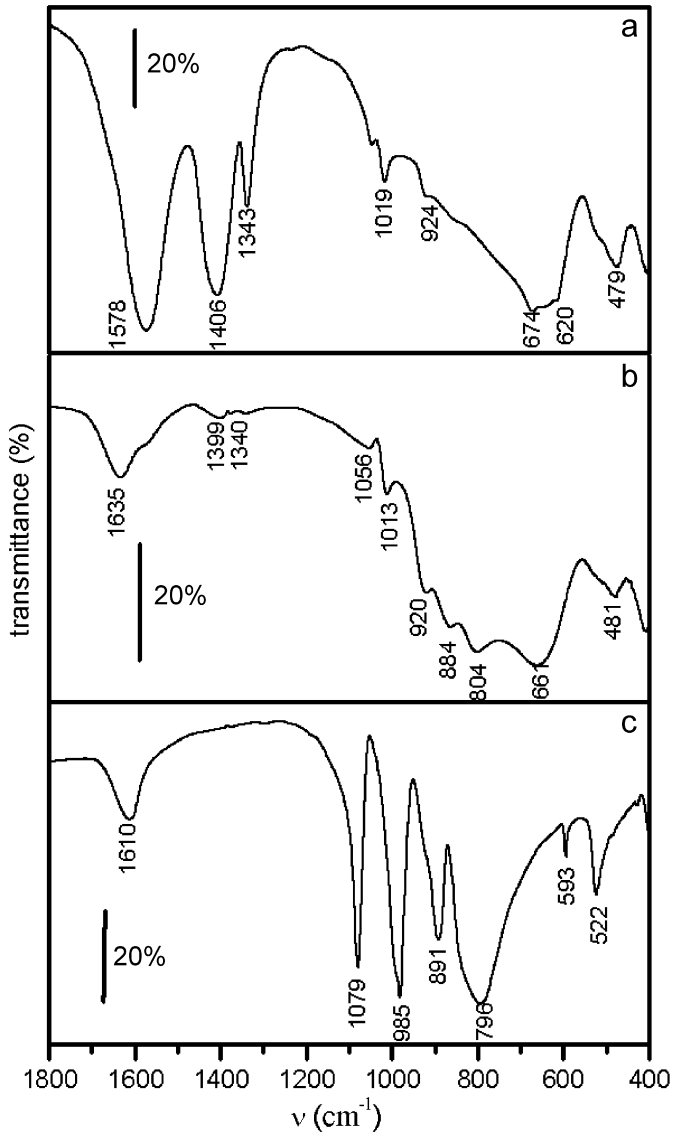


**Fig. 7.** FT-IR spectra (KBr disks) of (a) (Ni,Zn)-hydroxyacetate, (b) intercalated Ni–Zn hydroxysalt NiZnPW3-72HT90 and (c) $Na_3PW_{12}O_{40}$.

conditions chosen were pH = 3, contact time with Keggin anion solutions 72 h and fresh $Na_3PW_{12}O_{40}$ solution was changed every 24 h. The PXRD diagrams and FT-IR spectra for these samples are similar to those recorded for the sample that had been submitted to hydrothermal treatment, but an important dissolution of the precursor hydroxyacetate could not be avoided and the yield of the reaction was very poor.

### 3.7. Study of the tungsten-rich layered compound, sample NiZnW3-72HT90

After the above-described experiments, we concluded that the optimum conditions to achieve the largest exchange between the tungstophosphate anion and the nickel–zinc hydroxyacetate salt are to keep the suspension and the solid in contact for 72 h at pH = 3, and then to submit the solid to hydrothermal treatment at 90 °C for 24 h. Under these conditions, a solid with $d_{001} = 9.62$ Å is obtained (the PXRD pattern is included in Fig. 5), with an almost negligible C content (see Table 1) and the largest tungsten content.

However, according to the formula of the starting (Ni,Zn)-hydroxyacetate, the expected W/Zn ratio should be 4, different from the value experimentally found (see Table 1). Moreover, the gallery height is not large enough to accommodate the assumed PW12 anion. The shortest van der Waals diameter for $XM_{12}O_{40}^{n}$-type ions is 9.9 Å, measured along the $C_2$-axis. If we assume the full thickness of the layer to be 4.8 Å (similar to the value reported for the width of brucite-like layers in hydrotalcites) and considering the Keggin ions located with the $C_2$-axis perpendicular to the layers, it results in a structure with an expected gallery height of 14.7 Å [27,28]. In our case, the experimental W/Zn ratio for sample NiZnW3-72HT90 is 1.38, lower than the expected value for total $PW_{12}O_{40}^{3-}$ intercalation. A lower value of the basal spacing can be due to intercalation of lacunary species, whose formation (via depolymerization of $PW_{12}O_{40}^{3-}$) could be favoured in the basic environment of the gallery. This behaviour is similar to that previously reported for intercalation of polyoxovanadate anions into hydrotalcite-like compounds [29] and Ni–Zn hydroxysalts [30]. The basic environment of the interlayer space is due to the buffer character of the hydroxysalt and permits the presence of species that are unstable at the initial pH.

Infrared spectroscopy is one of the most effective means for characterizing the structure of Keggin-type polyoxometalates. The four characteristic bands of these species, $\nu_{as}$(P–$O_a$), $\nu_{as}$(M=$O_d$), $\nu_{as}$(M–$O_b$–M) and $\nu_{as}$(M–$O_c$–M), are extensively used to identify whether newly synthesized compounds contain Keggin-structure anions or not. The FT-IR spectra of the tungstophosphate-intercalated sample prepared at pH = 3 for 72 h and hydrothermally treated at 90 °C, and of $Na_3PW_{12}O_{40}$ are included in Fig. 7. A summary of positions of the most significant bands for these samples and for lacunary species is included in Table 2. The band at 1079 $cm^{-1}$ in the spectrum of reference compound $Na_3PW_{12}O_{40}$ (Fig. 7c) is attributed to the antisymmetric stretching mode of the central $PO_4$ tetrahedron $\nu_{as}$(P–O), the band at 985 $cm^{-1}$ to a stretching mode of W=$O_d$ and the bands at 891 and 796 $cm^{-1}$ to modes $\nu_{as}$(W–$O_b$–W) and $\nu_{as}$(W–$O_c$–W), respectively.

The spectrum of the intercalated sample (Fig. 7b) shows important changes with respect to the parent material: the characteristic bands of the acetate anion, due to the symmetric and antisymmetric vibration modes of the carboxylate group at 1406 and 1578 $cm^{-1}$, as well as the band due to the deformation mode of the $CH_3$ group at 1343 $cm^{-1}$, have almost disappeared. Furthermore, bands corresponding to the tungstophosphate anion with the Keggin structure (between 1100 and 700 $cm^{-1}$) are clearly observed [31,32]. Splitting of the band assigned to the vibration mode P–$O_a$ (1056 and 1013 $cm^{-1}$) is observed in the spectrum of the intercalated sample NiZnPW3-72HT. This splitting is characteristic of lacunary species (PW11 and PW9). The intensities of the bands decrease, and a shift of the band due to the vibration mode $\nu$W=$O_d$ (920 $cm^{-1}$) to lower wavenumbers, owing to interaction of the Keggin anion with the layer, is observed. Cation–anion interaction and hydrogen bonding draw electron density away from the metal-oxygen bonds and decrease their stretching wavenumbers. This fact has been previously

**Table 2**
FTIR data ($cm^{-1}$) of some tungstophosphate(V) anions, $Na_3PW_{12}O_{40}$ salt and NiZnW3-72HT90 sample here studied

| Sample | $\nu$P–$O_a$ | $\nu$W=$O_d$ | $\nu$W–$O_b$–W | $\nu$W–$O_c$–W |
|---|---|---|---|---|
| $PW12O40^{3-}$ | 1079 | 983 | 890–850 | 800–760 |
| $PW11O39^{7-}$ | 1095,1043 | 953 | 862–833 | 805–730 |
| $PW_9O_{34}^{9-}$ | 1052,1017 | 941 | 886–836 | 760–740 |
| $Na_3PW_{12}O_{40}$ | 1079 | 985 | 891 | 796 |
| NiZnW3-72HT90 | 1056,1013 | 920 | 884 | 804 |

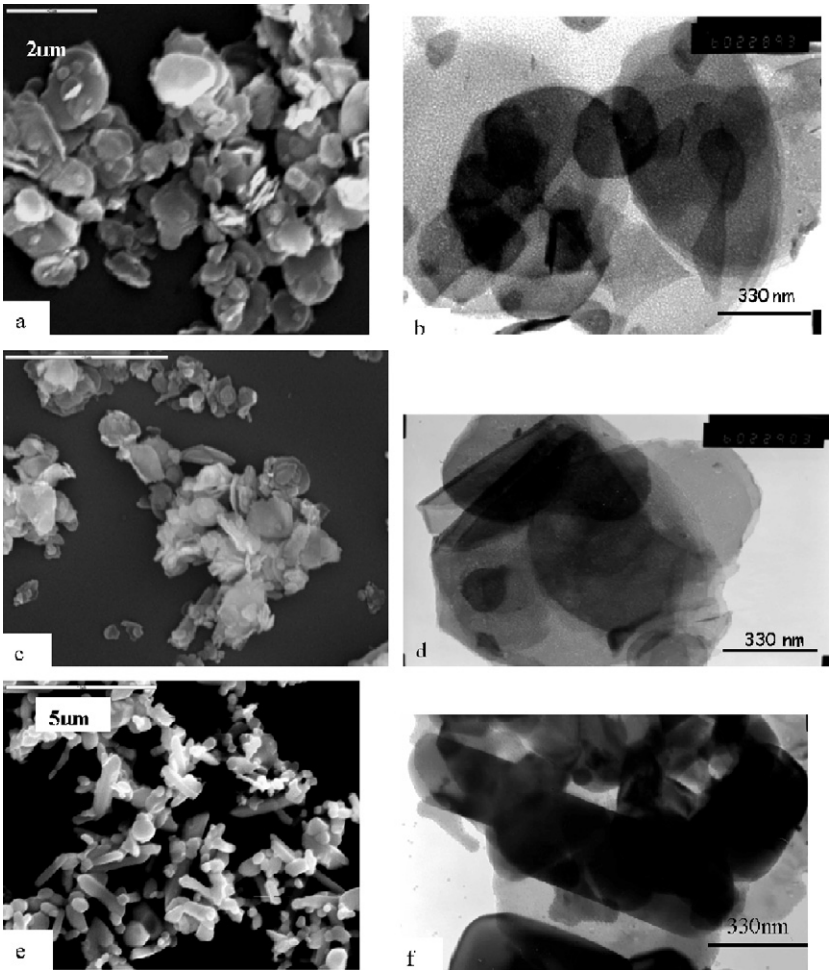


**Fig. 8.** SEM and TEM micrographs of sample NiZnPW3-72HT90: (a, b) uncalcined sample, (c, d) calcined at 250 °C and (e, f) calcined at 1000 °C.

observed by other authors and has been attributed to the interaction of Keggin anions with the solvent or with a silica matrix [11,32]. The overall observed decrease in the intensities of the characteristic bands can be attributed to the formation of hydrogen bond bridges between polyoxotungstate units and hydroxyl groups in the layer [33]. From FT-IR data in Table 2, we can suggest PW11 and PW9 as the most probable anions in the interlayer space, they might be formed by the removal of one or three octahedra, respectively, from the PW12 unit at high pH (Fig. 4). If these were the actual intercalated species, from its formal charge, the expected W/Zn molar ratio would be 1.57 for PW11 and 1 for PW9, closer to the experimental value (1.38) than that corresponding to the intercalation of unmodified PW12 units. However, the size of these anions is still larger than the measured basal spacing; so to accommodate these anions in the interlayer gallery, a grafting process should take place. Wang et al. [15] have proposed that intercalation of polyoxotungstate species into LDH takes place via a grafting process, to explain the small values of $d_{001}$ observed. This argument was also used to explain the intercalation of polyoxovanadate into (Ni, Zn) hydroxyacetate [30]. This process is produced by the elimination of OH groups from the layer, and oxygen atoms from the polyoxometalate units are located in their places, therefore leading to a decrease in the basal spacing.

SEM and TEM photographs included in Fig. 8a and b show the presence of plate-like particles, similar to the parent Ni–Zn hydroxyacetate (Fig. 3), suggesting a topotactic exchange reaction; the size is small ($<2\,\mu m$) and their edges or borders are broken due to the extreme conditions under which they were prepared and treated (acid pH and hydrothermal treatment).

TG and DTA curves and mass spectrometry diagrams for sample NiZnW3-72HT90 are shown in Fig. 9. The thermal decomposition proceeds mainly in two steps, with a broad endothermic effect in the DTA curve centred around 150 °C with a simultaneous weight loss of ca. 5.4% of the original sample weight. This effect is due to the removal of interlayer water molecules (detected as a signal at $m/z = 18$ due to $H_2O^+$). The second weight loss, between 200 and 550 °C, is assigned to the removal of hydroxide groups from the layer, condensed to form water molecules, and corresponds to 11.8% of the original sample weight, identified by mass spectroscopy by the expected signal for $H_2O^+$. Finally, a small weight loss (ca. 0.9%) up to 600 °C is observed, which can be due to the loss of phosphorous oxide ($m/z = 63$ and 79 corresponding to $PO_2^+$ and $PO_3^+$ ionic species, respectively). In general, the products formed upon thermal decomposition of this type of layered compounds [7,30,34] are simple and mixed oxides with the spinel structure. The potential application of this type of mixed oxides will depend on their precise composition and structure. Here, we have identified the nature and morphology of calcinated products of the NiZnW3-72HT90 sample at different temperatures by PXRD and electron microscopy.

The PXRD diagrams for the solids calcined at different temperatures are included in Fig. 10. No major changes are observed in the PXRD diagram, where the position of the line due to diffraction by (001) planes shifts from 9.56° to 11.04° ($2\theta$) and

the other basal lines disappear. The peak at ca. 60° ($d = 1.532$ Å) assigned to diffraction by (110) planes also remains unchanged. This last peak is characteristic of the layered structure, pointing out that the intercalated compound is stable at 250 °C. After calcination at 250 °C the solid retains the external shape of the parent material, as can be observed in SEM and TEM photographs (Fig. 8c and d). On the other hand, calcination at 500 °C (micrograph not shown) leads to the destruction of the layered structure, and only broad peaks, whose positions do not coincide with any of the lines previously recorded, are observed in the PXRD pattern. These new peaks are due to diffraction by NiO, with the rock salt structure. The plate-like particles in the photograph are similar to the parent materials, but less rounded in shape and they appear broken due to dehydroxylation of the layers. The PXRD diagram of the sample calcined at high temperature, ca. 1000 °C (Fig. 10), shows the peaks of the NiO (JCPDS pattern 4-835) and other peaks corresponding to a monoclinic phase of tungstate salt. The diffraction lines of the monoclinic phase are located between those corresponding to $NiWO_4$ (pattern 15-755) and $ZnWO_4$ (pattern 15-774), which suggests the formation of a (Zn, Ni)$WO_4$ solid solution. Phosphorous-containing phases are not identified in any case due to its loss as a volatile oxide at 420 °C (besides the P content is too low to be identified as a phosphate phase by PXRD). A separate ZnO phase is not identified either, so we should conclude that all Zn should be included in the monoclinic tungstate phase. It should be remembered that the Ni/Zn/W molar ratio in the original sample was 0.82/0.36/0.50, and so an excess of nickel over zinc exists. The remaining nickel is identified as NiO. The SEM photograph included in Fig. 8e shows small particles and important changes in the shape after calcination at 1000 °C. A sinterization process has taken place as evidenced by the dark particles in the TEM photograph included in Fig. 8f.

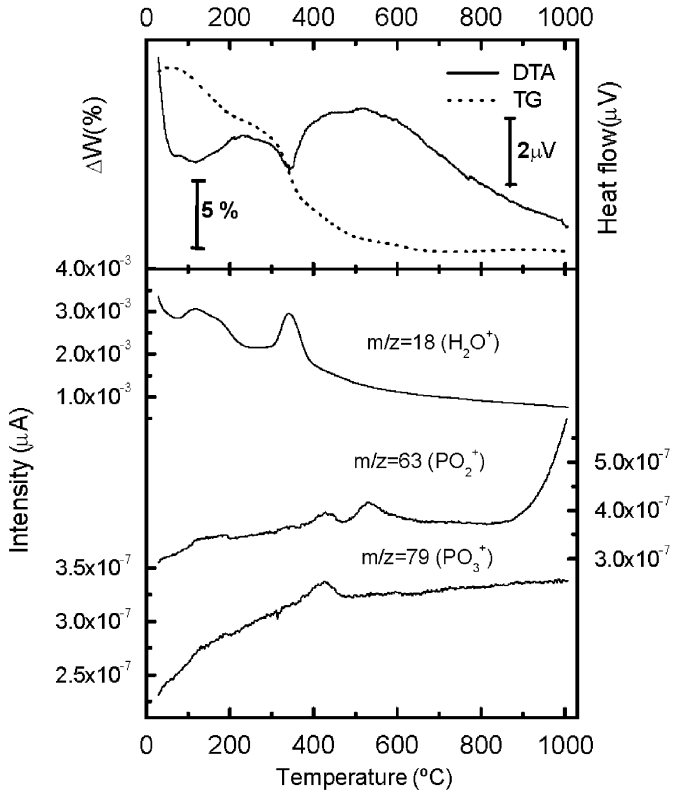


**Fig. 9.** DTA/TG curves recorded in $N_2$ and mass spectrometry diagrams for sample NiZnPW3-72HT90.

## 4. Conclusions

Anion exchange reactions of acetate LHS-Ni–Zn with lacunary tungstophosphate(V) anions were carried out and as the precursor structure has been maintained the process could be considered topotactic. The optimum conditions to reach a maximum content of W (ca. 48%) in the layered compound were pH = 3, exchange time 72 h and hydrothermal treatment at 90 °C for 24 h. From the experimental results reported so far, the species $PW_{11}O_{39}^{7-}$ and $PW_9O_{34}^{9-}$ can be suggested as those that actually exist in the interlayer. Grafting of the lacunary species onto the hydroxyl layers is favoured, probably due to partial dissolution of the layers under the acidic conditions.

The compound with intercalated tungstophosphate is stable up to 250 °C, with a decrease in the gallery height due to loss of interlayer water. The dehydroxylation causes the collapse of the structure and removal of hydroxyl groups through condensation to produce water vapour, as well as small amounts of phosphor-

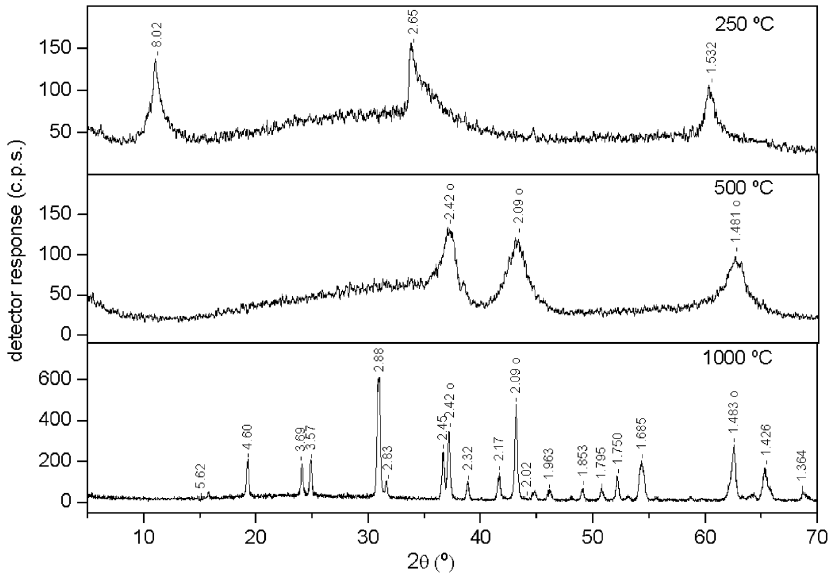


**Fig. 10.** PXRD diagram of sample NiZnPW3-72HT90 calcined at the given temperatures; (o) NiO (rock salt), unlabelled peaks correspond to a monoclinic $MWO_4$ phase.

ous oxide. Therefore, the solid obtained at 500 °C shows a PXRD diagram characteristic of mostly amorphous phases that crystallize at higher temperatures to yield NiO (with the rock salt structure) and a $Zn_{1-x}Ni_xWO_4$ solid solution, the value of $x$ depending on the composition of the parent hydroxyacetate.

## Acknowledgments

The authors thank MCyT (MAT2003-06605-C02 Project) and Junta de Andalucia (Grupo FQ214) for financial support.

## References

[1] V. Rives (Ed.), Layered Double Hydroxides: Present and Future, Nova Science Publishers, Inc., New York, 2001.
[2] X. Duan, D.G. Evans (Eds.), Layered Double Hydroxides, series ed. D.M.P. Mingos V, Structural and Bonding, 2006.
[3] V. Rives, M.A. Ulibarri, Coord. Chem. Rev. 181 (1999) 61–120.
[4] S. Brito, J.T. Rajamathi, N. Ravishankar, C. Shivakumara, M. Rajamathi, Solid State Sci. 8 (2006) 162–167.
[5] M. Taibi, S. Ammar, N. Jouini, F. Fiévet, J. Phys. Chem. Solids 67 (2006) 932–937.
[6] S.P. Newman, W. Jones, J. Solid State Chem. 148 (1999) 26–40.
[7] R. Rojas, C. Barriga, M.A. Ulibarri, P. Malet, V. Rives, J. Mater. Chem. 12 (2002) 1071–1078.
[8] E. Kandare, J.M. Hossenlopp, J. Phys. Chem. B 109 (2005) 8469–8475.
[9] M.T. Pope, A. Müller, Angew. Chem. Int. Ed. Engl. 30 (1991) 34–48.
[10] I.V. Kozhevnikov, J. Mol. Catal. A 262 (2007) 86–92.
[11] D. Li, Y. Guo, C. Hu, L. Mao, E. Wang, Appl. Catal. A—Gen. 235 (2002) 11–20.
[12] X. Qu, Y. Guo, C. Hu, J. Mol. Catal. A 262 (2007) 128–135.
[13] Y. Guo, D. Li, C. Hu, E. Wang, Y. Zou, H. Ding, S. Feng, Microp. Mesop. Mater. 56 (2002) 153–162.
[14] L.R. Pizzio, C.V. Cáceres, M.N. Blanco, Appl. Surf. Sci. 151 (1999) 91–101.
[15] J. Wang, Y. Tian, R. Wang, A. Clearfield, Chem. Mater. 4 (6) (1992) 1276–1282.
[16] J.D. Wang, J.G. Serrette, Y. Tian, A. Clearfield, Appl. Clay Sci. 10 (1995) 103–115.
[17] S.K. Yun, T.J. Pinnavaia, Inorg. Chem. 35 (1996) 6853–6860.
[18] E.M. Serwicka, P. Nowak, K. Bahranowski, W. Jones, F. Kooli, J. Mater. Chem. 7 (9) (1997) 1937–1939.
[19] M. del Arco, D. Carriazo, S. Gutiérrez, C. Martin, V. Rives, Inorg. Chem. 43 (2004) 375–384.
[20] D. Carriazo, C. Domingo, C. Martin, V. Rives, Inorg. Chem. 45 (2006) 1243–1251.
[21] S. Yamanaka, K. Ando, M. Ohashi, Mater. Res. Soc. Symp. Proc. 371 (1995) 131–142.
[22] L. Poul, N. Jouini, F. Fiévet, Chem. Mater. 12 (2000) 3123–3132.
[23] K. Nakamoto, Infrared and Raman Spectra of Inorganic and Coordination Compounds, fourth ed, Wiley, New York, 1986.
[24] J.-H. Choy, Y.M. Kwon, K.S. Han, S.-W. Song, S.H. Chang, Mater. Lett. 34 (1998) 353–356.
[25] M.T. Pope, Heteropoly and Isopoly Oxometalates, Springer, Berlin, 1983.
[26] H. Nishizawa, K. Yvasa, J. Solid State Chem. 141 (1998) 229–334.
[27] J. Wang, Y. Tian, R.-C. Wang, J.L. Colón, A. Clearfield, in: R.L. Bedard, T. Bein, M.E. Davis, J. Garces, V.A. Maroni, G.D. Stucky (Eds.), Synthesis/Characterization and Novel Applications on Molecular Sieve Materials, Materials Research Society, Pittsburgh, 1991, pp. 63–80.
[28] T. Kwon, T.J. Pinnavaia, Chem. Mater. 4 (1989) 381–383.
[29] C. Barriga, W. Jones, P. Malet, V. Rives, M.A. Ulibarri, Inorg. Chem. 37 (1998) 1812–1820.
[30] R. Rojas, C. Barriga, M.A. Ulibarri, V. Rives, J. Solid State Chem. 177 (2004) 3392–3401.
[31] Y. Guo, Y. Wang, C. Hu, Y. Wang, E. Wang, Chem. Mater. 12 (2000) 3501–3508.
[32] R. Thouvenot, M. Fournier, C. Rocchiccioli-Deltcheff, J. Chem. Soc. Faraday Trans. 87 (1991) 2829–2835.
[33] Y. Guo, D. Li, C. Hu, Y. Wang, E. Wang, Int. J. Inorg. Mater. 3 (2001) 347–355.
[34] E. Gardner, T.J. Pinnavaia, Appl. Catal. A 167 (1998) 65–74.